Cell

Endothelial-Derived Angiocrine Signals Induce and Sustain Regenerative Lung Alveolarization

Bi-Sen Ding,[1] Daniel J. Nolan,[1] Peipei Guo,[1] Alexander O. Babazadeh,[1] Zhongwei Cao,[1] Zev Rosenwaks,[2] Ronald G. Crystal,[1] Michael Simons,[3] Thomas N. Sato,[4] Stefan Worgall,[1] Koji Shido,[1] Sina Y. Rabbany,[1,5] and Shahin Rafii[1,*]

[1]Howard Hughes Medical Institute, Ansary Stem Cell Institute, Department of Genetic Medicine
[2]Ronald O. Perelman and Claudia Cohen Center for Reproductive Medicine
Weill Cornell Medical College, New York, NY 10065, USA
[3]Section of Cardiovascular Medicine, Yale University School of Medicine, New Haven, CT 06510, USA
[4]Graduate School of Biological Sciences, Nara Institute of Science and Technology, Ikoma, Nara 630-0192, Japan
[5]Bioengineering Program, Hofstra University, Hempstead, NY 11549, USA
*Correspondence: srafii@med.cornell.edu
DOI 10.1016/j.cell.2011.10.003

SUMMARY

To identify pathways involved in adult lung regeneration, we employ a unilateral pneumonectomy (PNX) model that promotes regenerative alveolarization in the remaining intact lung. We show that PNX stimulates pulmonary capillary endothelial cells (PCECs) to produce angiocrine growth factors that induce proliferation of epithelial progenitor cells supporting alveologenesis. Endothelial cells trigger expansion of cocultured epithelial cells, forming three-dimensional angiospheres reminiscent of alveolar-capillary sacs. After PNX, endothelial-specific inducible genetic ablation of *Vegfr2* and *Fgfr1* in mice inhibits production of MMP14, impairing alveolarization. MMP14 promotes expansion of epithelial progenitor cells by unmasking cryptic EGF-like ectodomains that activate the EGF receptor (EGFR). Consistent with this, neutralization of MMP14 impairs EGFR-mediated alveolar regeneration, whereas administration of EGF or intravascular transplantation of MMP14$^+$ PCECs into pneumonectomized *Vegfr2/Fgfr1*-deficient mice restores alveologenesis and lung inspiratory volume and compliance function. VEGFR2 and FGFR1 activation in PCECs therefore increases MMP14-dependent bioavailability of EGFR ligands to initiate and sustain alveologenesis.

INTRODUCTION

Defining the cellular and molecular mechanisms that modulate lung regeneration is essential to develop strategies to treat respiratory disorders (Beers and Morrisey, 2011; Chapman, 2011; Metzger et al., 2008; Morris et al., 2003; Morrisey and Hogan, 2010; Warburton et al., 2010). To identify regulatory mechanisms involved in adult lung regeneration, we employed a model in which surgical removal of the left lung, known as left unilateral pneumonectomy (PNX), induces the expansion of mass and volume in the intact lobes of remaining right lung (Cowan and Crystal, 1975; Leuwerke et al., 2002; Nolen-Walston et al., 2008). This regenerative process is driven by alveologenesis, a process that is dependent on proliferation of epithelial progenitor cells (Kotton and Fine, 2008; Rock and Hogan, 2011; Stripp and Reynolds, 2008), which comprise subsets of alveolar epithelial cells (AECs) (Chapman et al., 2011; Liu et al., 2011) and presumably bronchioalveolar stem cells (BASCs) (Kim et al., 2005; Zhang et al., 2008). However, the precise mechanism(s) by which PNX initiates and sustains regenerative alveologenesis is unknown.

During lung development, the vascular plexus (capillary) sprouts in parallel with the alveolar budding (Cardoso, 2001; Metzger et al., 2008; White et al., 2007). As a unique organ that facilitates gas exchange, the lung alveolus is highly vascularized, with pulmonary capillary endothelial cells (PCECs) lining all alveoli and residing in proximity to AECs (Bhattacharya, 2005; Komarova and Malik, 2010; Muzykantov, 2005; Petrache et al., 2005; Voelkel et al., 2006). The formation of the alveolar-capillary interface is pivotal for pulmonary gas exchange function (Giordano et al., 2008; Huh et al., 2010; Petersen et al., 2010; Vaporciyan et al., 1993). However, the role of PCECs as a specialized capillary vasculature in guiding alveolarization (DeLisser et al., 2006; Leuwerke et al., 2002), in particular during regenerative alveolar remodeling (Metzger et al., 2008), remains unknown.

Capillary endothelial cells (ECs) that form the building blocks of microvasculature of individual organs are endowed with organ-specific phenotypic and functional attributes (Aird, 2007; Carmeliet, 2005; Red-Horse et al., 2007; Ruoslahti and Rajotte, 2000). Capillary ECs are not solely passive conduits for the delivery of oxygen or nutrients; they also support organ development (Lammert et al., 2001; Matsumoto et al., 2001; Sakaguchi et al., 2008) and adult organ regeneration through elaboration

of tissue-specific paracrine growth factors, defined as angiocrine factors (Butler et al., 2010a, 2010b).

For example, sinusoidal endothelial cells (SECs) within liver and bone marrow (BM) comprise phenotypically and functionally discreet populations of ECs. We have shown that, after partial hepatectomy, liver SECs (LSECs) through a process of ''inductive angiogenesis''—that is, via angiocrine production of hepatocyte growth factor and Wnt2—stimulate hepatocyte proliferation (Ding et al., 2010). Subsequently, LSECs undergo ''proliferative (sprouting) angiogenesis'' to meet the incremental demand in blood supply to regenerating liver tissue. Similarly, after chemotherapy and irradiation, activated BM SECs reconstitute hematopoiesis by angiocrine expression of Notch ligands and IGFBPs (Butler et al., 2010b; Kobayashi et al., 2010). Conditional deletion of VEGF-A receptor-2 (VEGFR2) in either LSECs (Ding et al., 2010) or BM SECs (Hooper et al., 2009) of the adult mice inhibits liver and BM regeneration by impairing the production of angiocrine factors, underscoring the physiological importance of endothelial-derived instructive signals in adult organ regeneration. These findings raise the possibility that PCECs also comprise a functionally unique population of specialized ECs, which by production of lung-specific angiocrine factors, induce regenerative alveolarization.

In addition to their enduring capacity to undergo proliferative sprouting angiogenesis to vascularize alveoli (Alvarez et al., 2008; Del Moral et al., 2006; Shu et al., 2002), PCECs specify the differentiation of endoderm and mesoderm progenitors into primitive lung epithelial and vascular precursor cells by producing paracrine factors (Bhattacharya, 2005; Yamamoto et al., 2007). These findings suggest that PCECs may promote alveologenesis by elaborating angiocrine growth signals. Whether PCEC-derived instructive signals can trigger regenerative alveolarization in the adult lungs has, however, not been studied. Indeed, the paucity of mouse lung regenerative genetic models and lack of operational definition of PCECs have handicapped studies of PCECs in guiding alveolar regeneration in adult lungs.

In this study, we have defined the phenotypic and operational markers of mouse PCEC population as VE-cadherin$^+$VEGFR2$^+$FGFR1$^+$CD34$^+$ ECs. We employ a unilateral pneumonectomy (PNX) model to investigate the role of PCECs in supporting alveolar regeneration. Surgical resection of the left lung, which does not perturb the vascular integrity of the remaining right lobes, induces regrowth of these residual lobes. Here, we demonstrate that PNX through activation of VEGFR2 and FGFR1 induces PCECs of the remaining right lobes to produce the angiocrine matrix metalloprotease MMP14. In turn, MMP14 promotes regenerative alveolarization by unmasking cryptic epidermal growth factor (EGF)-like ligands that stimulate proliferation of epithelial progenitor cells. These data suggest that PCECs could be therapeutically exploited for the treatment of lung disorders.

RESULTS

PNX Induces Expansion of Epithelial Progenitor Cells

Within 15 days after PNX, there is a dramatic regeneration in the mass and volume of remaining right lung lobes (Figures 1A and 1B). Lung epithelial progenitor cells, including subsets of BASCs identified by Clara cell-secreted protein (CCSP)$^+$pro-surfactant protein C (SPC)$^+$Sca-1$^+$ (CCSP$^+$SPC$^+$Sca-1$^+$) cells and type II AECs (AECIIs) by SPC$^+$E-cadherin$^+$ cells contribute to alveolar epithelialization (Beers and Morrisey, 2011). To determine the contribution of epithelial progenitor cells to lung regeneration, after PNX, we introduced BrdU in drinking water to detect slow-cycling cells. On day 3 after PNX, we observed amplification of BrdU$^+$CCSP$^+$ cells at bronchioalveolar duct junction (BADJ) (Figure 1C). To track expansion of BrdU$^+$CCSP$^+$ cells, we used reporter transgenic mice in which *CCSP* and *SPC* promoters drive YFP expression (*CCSP-YFP* and *SPC-YFP* mice) (Perl et al., 2002) (Figures 1D and 1E). We performed polyvariate flow cytometric analysis of all mononuclear cells in regenerating lungs on day 3 after PNX. The CCSP$^+$BrdU$^+$ cells localized to the BADJ region were CCSP$^+$SPC$^+$Sca-1$^+$VE-cadherin$^-$CD31$^-$ cells, a phenotypic signature observed on BASCs (Kim et al., 2005). At this early time point, we did not detect proliferation of SPC$^+$Sca-1$^-$CCSP$^-$ AECIIs or VE-cadherin$^+$CD31$^+$ PCECs. Therefore, PNX induces expansion of slow-cycling CCSP$^+$SPC$^+$Sca-1$^+$ BASC-like cells in early phases of lung regeneration, when there is minimal proliferation of AECs and PCECs.

PNX Stimulates Expansion of PCECs and AECs Colocalizing at the Alveolar-Capillary Interface

To identify time points after PNX when AECs and PCECs undergo significant proliferation, we examined the kinetics of incorporation of intraperitoneally injected BrdU in the remaining lobes and found a global appearance of transit amplifying cells (TACs) that peaked at day 7 after PNX (Figure 2A and Figure S1 available online). In sham operated mouse lungs, there was little uptake of BrdU. To characterize cell types in TACs on day 7 after PNX, we performed PNX on *SPC-YFP* reporter mice. There was increased proliferation of SPC$^+$ cells that coexpress pro-surfactant protein D (SPD) and E-cadherin, markers representing AECIIs (Beers et al., 1994; Whitsett et al., 2010) (Figure 2B).

The remaining SPC$^-$ TACs consist of small fraction of CCSP$^+$ airway Clara cells (Rawlins et al., 2009) and VE-cadherin$^+$ PCECs. Analysis of BrdU incorporation showed that, on day 7 after PNX, proliferating VE-cadherin$^+$CD34$^+$FGFR1$^+$VEGFR2$^+$CD45$^-$ PCECs accounted for 7% of mononuclear cells (Figure 2C), which were localized to the vicinity of SPC$^+$ AECIIs (Figure 2D). Using SPC$^+$E-cadherin$^+$ and VE-cadherin$^+$CD34$^+$ as operational markers for AECIIs and PCECs, respectively, we found that, on day 15, after PNX there was a 3-fold increase in the population of both AECIIs and PCECs (Figure 2E). Therefore, after PNX, the increase in lung mass and volume is due to proliferation of PCECs and epithelial progenitor cells, with BASC-like cells expanding at early time point (day 3) and AECIIs proliferating at later time points (Figure 2F).

Sequential Activation of VEGFR2 and FGFR1 in PCECs Is Essential for Functional Alveolar Regeneration

One mechanism by which PNX initiates lung regeneration could be through activation of PCECs to produce epithelial-active angiocrine factors. As VEGFR2, the principal tyrosine kinase receptor of VEGF-A, plays a critical role in induction of angiocrine

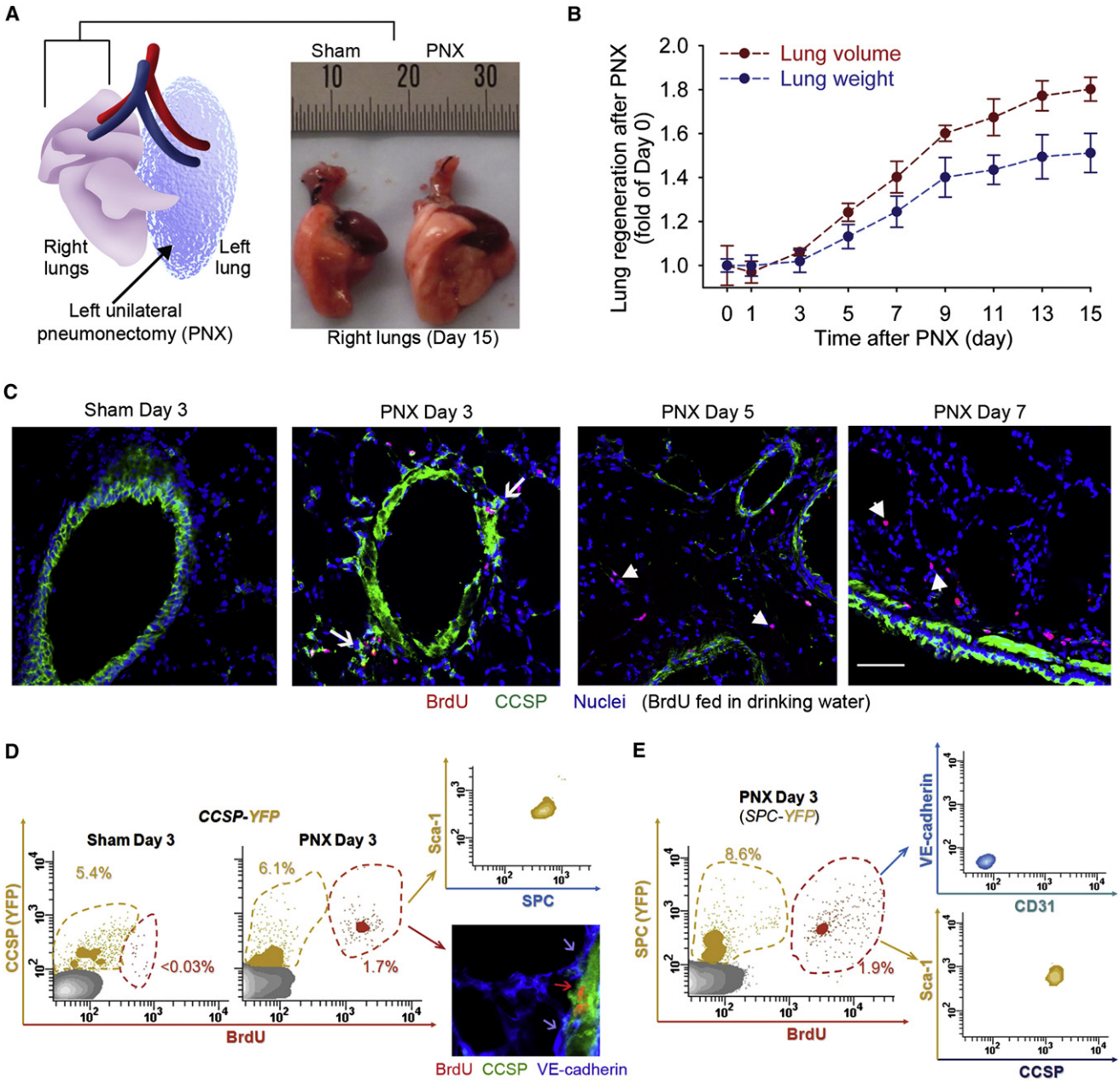

Figure 1. PNX Induces Right Lung Regeneration and Expansion of Lung Epithelial Progenitors

(A and B) Restoration of weight and volume in the remaining intact right lung lobes after resection of left lung. (A) Schema illustrating PNX procedure and representative image of regenerated right lungs 15 days after PNX. (B) Lung regeneration is initiated 3 days after PNX and achieves its maximum size and volume at day 15. n = 5.

(C) Amplification of CCSP$^+$ cells at bronchioalveolar duct junction (BADJ) on day 3 after PNX. Mice were fed with BrdU-containing drinking water to pulse proliferating lung progenitors. There is a specific expansion of CCSP$^+$BrdU$^+$ cells localized at BADJ on day 3 after PNX (arrows). Note the distribution of BrdU$^+$ cells in distal alveolar space thereafter (arrowheads).

(D and E) CCSP$^+$SPC$^+$Sca-1$^+$VE-cadherin$^-$CD31$^-$ BASC-like cells were identified and quantified in *CCSP-YFP* and *SPC-YFP* mice 3 days after PNX. There is minimal BrdU uptake in VE-cadherin$^+$CD31$^+$ PCECs, indicating that, at this time point, PCECs do not undergo proliferation. Note the close cellular juxtaposition of VE-cadherin$^+$ PCECs (blue arrow) and proliferating CCSP$^+$BrdU$^+$ BASCs (red arrow) in the lower inset of (D).

factors (Ding et al., 2010; Hooper et al., 2009), we analyzed the activation of VEGFR2 in PCECs after PNX. Although VEGFR2 protein level in PCECs is unaltered, after PNX, the extent of phosphorylated VEGFR2 is increased, indicating activation of this VEGF-A receptor in the ECs of regenerating right lobes (Figure 3A).

Because FGFR1 is expressed in PCECs and can reciprocally modulate the expression and activation state of VEGFR2

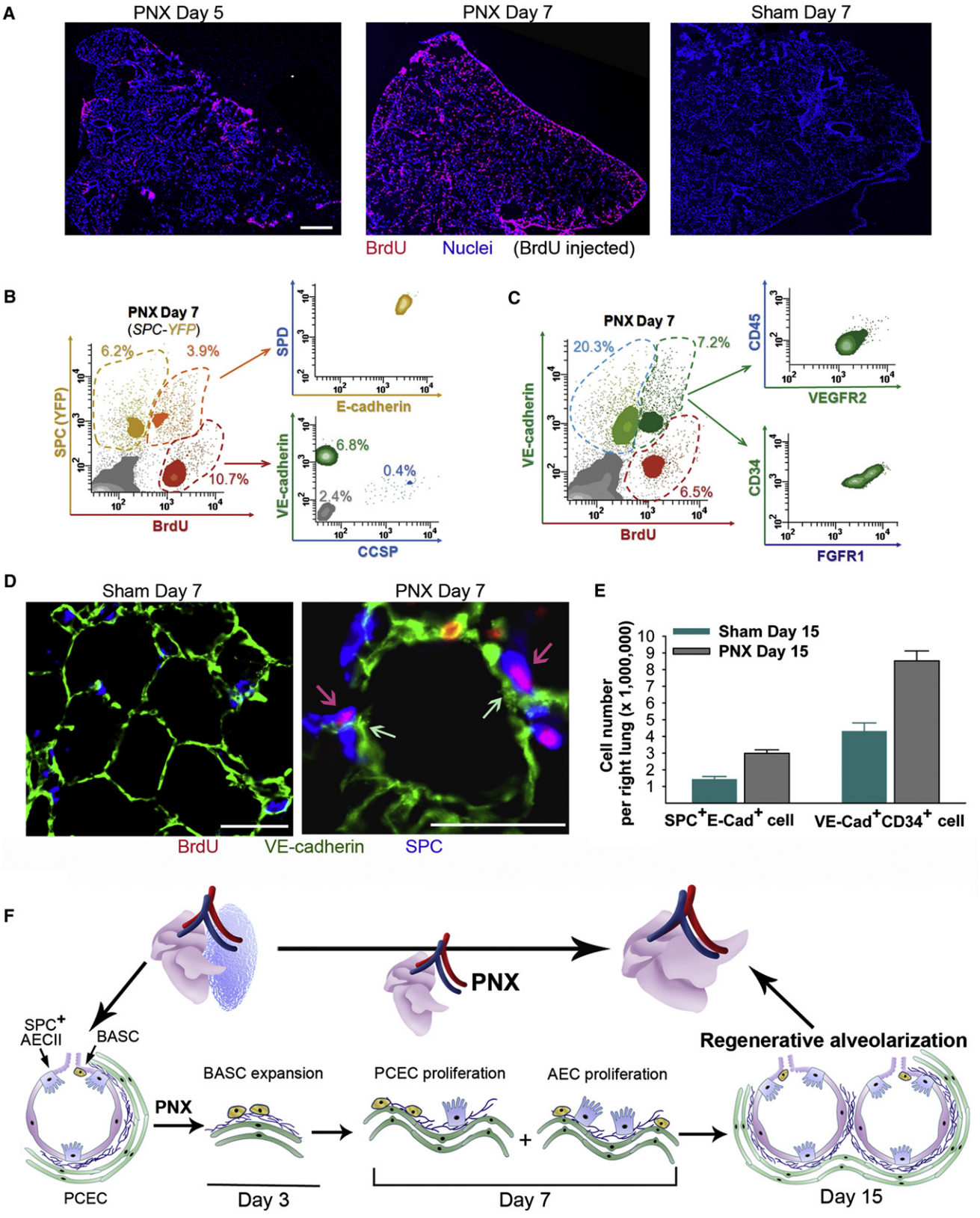
A
PNX Day 5
PNX Day 7
Sham Day 7
BrdU
Nuclei
(BrdU injected)
B
PNX Day 7
(SPC-YFP)
6.2%
3.9%
10.7%
SPC (YFP)
BrdU
SPD
E-cadherin
VE-cadherin
6.8%
0.4%
2.4%
CCSP
C
PNX Day 7
20.3%
7.2%
6.5%
VE-cadherin
BrdU
CD45
VEGFR2
CD34
FGFR1
D
Sham Day 7
PNX Day 7
BrdU
VE-cadherin
SPC
E
Sham Day 15
PNX Day 15
Cell number per right lung (x 1,000,000)
SPC+E-Cad+ cell
VE-Cad+CD34+ cell
F
PNX
SPC+ AECII
BASC
PCEC
BASC expansion
PNX
Day 3
PCEC proliferation
AEC proliferation
Day 7
Regenerative alveolarization
Day 15

(Murakami et al., 2011; White et al., 2007) to drive angiocrine factor production, we also studied the expression of FGFR1 by PCECs. After PNX, FGFR1 protein was upregulated in a time-dependent manner. Thus, whereas in early phases of lung regeneration, activation of VEGFR2 in PCECs initiates alveologenesis, at later phases, coactivation of FGFR1 might synergize with VEGFR2 to sustain regenerative epithelialization.

To elucidate the endothelial-specific function of VEGFR2 and FGFR1 in the lungs, we employed an inducible knockout strategy to selectively delete the *Vegfr2* gene in adult mouse ECs (Figure 3B), using transgenic mice in which the *VE-cadherin* promoter drives expression of tamoxifen-responsive Cre *(VE-Cad-CreERT2)* (Wang et al., 2010). Tamoxifen treatment selectively deletes *Vegfr2* in ECs (*Vegfr2*$^{i\Delta EC/i\Delta EC}$ mice). To account for off-target toxicity by CreERT2, we used heterozygous *Vegfr2*-deficient (*Vegfr2*$^{i\Delta EC/+}$) mice as control. We also generated mice in which both *Vegfr2* and *Fgfr1* were deleted in ECs. However, because these mice could not tolerate surgical procedures because of vascular instability, we investigated the role of coactivation of FGFR1 and VEGFR2 in supporting alveologenesis by inducible *Vegfr2* and partial *Fgfr1* deletion in ECs (*Vegfr2*$^{i\Delta EC/i\Delta EC}$*Fgfr1*$^{i\Delta EC/+}$ mice).

Before PNX, *Vegfr2*$^{i\Delta EC/i\Delta EC}$ and *Vegfr2*$^{i\Delta EC/i\Delta EC}$*Fgfr1*$^{i\Delta EC/+}$ mice did not manifest alterations in lung mass or function (Figure S2). By contrast, on day 3 after PNX, proliferation of CCSP$^+$ Sca1$^+$ BASC-like cells was abolished in *Vegfr2*$^{i\Delta EC/i\Delta EC}$ mice (Figures 3C and S2), whereas there was no further inhibition in expansion of these cells in *Vegfr2*$^{i\Delta EC/i\Delta EC}$*Fgfr1*$^{i\Delta EC/+}$ mice after PNX. These data establish the critical role of VEGFR2 activation in supporting epithelialization at early phases of lung regeneration.

We then studied the role of VEGFR2 and FGFR1 coactivation in amplification of PCECs and AECIIs. Costaining of regenerating lungs with BrdU, VE-cadherin, and SPC at day 7 indicated that endothelial-specific knockdown of *Vegfr2* in mice (*Vegfr2*$^{i\Delta EC/i\Delta EC}$) abrogated propagation of both PCECs and AECIIs (Figures 3D and 3E). Notably, endothelial-specific knockdown of *Vegfr2* and *Fgfr1* (*Vegfr2*$^{i\Delta EC/i\Delta EC}$*Fgfr1*$^{i\Delta EC/+}$) further abolished proliferation of PCECs and AECIIs at this time point, suggesting that FGFR1 synergizes with VEGFR2 in stimulating PCECs to support AECII amplification and neoangiogenesis.

Deletion of *Vegfr2* and *Fgfr1* in PCECs Impairs Restoration of Alveolar Structure and Function

To determine whether coactivation of VEGFR2 and FGFR1 plays a role in improving lung function, we examined inspiratory volume and static compliance in *Vegfr2*$^{i\Delta EC/i\Delta EC}$*Fgfr1*$^{i\Delta EC/+}$ and control mice before and after PNX. These parameters of pulmonary function provide physiologically relevant indices of respiratory capacity. The restoration of pulmonary function after PNX was significantly impaired in *Vegfr2*$^{i\Delta EC/i\Delta EC}$*Fgfr1*$^{i\Delta EC/+}$ mice at a time point when control mice exhibited complete recovery (Figure 3F). Similarly, restoration of lung mass, volume, and cell expansion after PNX were all impaired in *Vegfr2*$^{i\Delta EC/i\Delta EC}$ *Fgfr1*$^{i\Delta EC/+}$ mice (Figure 3G). These data indicate that, after PNX, nonproliferating VE-cadherin$^+$ ECs induce early expansion of BASC-like cells via VEGFR2 activation. At later phases after PNX, upregulation of FGFR1 in conjunction with VEGFR2 activates PCECs to instruct epithelialization as well as vascular sprouting, restoring respiratory capacity (Figure 3H). Thus, PCECs produce angiocrine factors and participate in angiogenesis fostering generation of functional respiratory alveolar units.

PNX Induces Specific Upregulation of MMP14 in PCECs Expanding Epithelial Progenitor Cells

To identify the inductive angiocrine cue that initiates epithelialization, we compared the gene expression profiles of the regenerative lungs (Table S1) and found that, among alveologenic factors, membrane-type 1 matrix metalloproteinase (MMP14) was specifically upregulated in PCECs of wild-type, but not *Vegfr2*$^{i\Delta EC/i\Delta EC}$ or *Vegfr2*$^{i\Delta EC/i\Delta EC}$*Fgfr1*$^{i\Delta EC/+}$, mice (Figure S3). Analysis of MMP14 protein level in the pneumonectomized lungs revealed its temporal upregulation that peaks at day 7 and levels off afterward (Figure 4A). Immunostaining and flow cytometric analysis illustrated the PCEC-specific localization of MMP14 after PNX, which was diminished in the *Vegfr2*$^{i\Delta EC/i\Delta EC}$ *Fgfr1*$^{i\Delta EC/+}$ lungs (Figures 4B and 4C). MMP14 was not upregulated in other vascular rich organs, including liver, heart, spleen, and kidney (Figure S3), indicating that, after PNX, MMP14 is selectively upregulated in VEGFR2- and FGFR1-activated PCECs.

To define the mechanism by which angiocrine expression of MMP14 promotes the propagation of epithelial progenitor cells, we isolated AECIIs and BASCs from *SPC-YFP* and *CCSP-YFP* mice, respectively, and cocultured with primary ECs. YFP expression was utilized to track their fate during coculture. The E4ORF1 gene, which through activation of the Akt pathway maintains angiocrine capacity, was introduced into primary ECs (Seandel et al., 2008, Kobayashi et al., 2010). Because MMP14 was upregulated in MAP kinase-activated ECs, we also introduced c-Raf to constitutively stimulate MAP kinase

Figure 2. At Day 7 after PNX, Expansion of AECs and PCECs Sustains Alveolar Regeneration

(A) After PNX, transit amplifying cells (TACs) were pulsed with i.p. administration of BrdU and revealed by BrdU staining. BrdU$^+$ TACs increased throughout the right lungs and peaked at day 7 after PNX. Scale bar, 2.5 mm.

(B and C) Quantification of TACs in the remaining right lungs at day 7 after PNX. Polyvariate flow cytometric analysis of total mononuclear cells demonstrated expansion of SPD$^+$SPC$^+$E-cadherin$^+$ AECIIs and VE-cadherin$^+$CD34$^+$VEGFR2$^+$FGFR1$^+$CD45$^-$ PCECs.

(D) Proliferation of SPC$^+$ AECIIs and VE-cadherin$^+$ PCECs at the alveolar-capillary interface in the remaining lungs at day 7 after PNX. Note the close cellular proximity between PCECs (green arrow) with BrdU$^+$ AECIIs (red arrow). Scale bar, 100 μm.

(E) Quantification of VE-cadherin$^+$CD34$^+$ PCECs and SPC$^+$E-cadherin$^+$ AECIIs in the remaining lungs 15 days after PNX; PNX induces proliferation of PCECs and AECs. n = 5.

(F) Proposed model for regenerative alveolarization mediated by proliferation of lung epithelial progenitors. PNX-induced alveolar regeneration is primarily mediated by amplification of BASCs, AECs, and PCECs.

See also Figure S1.

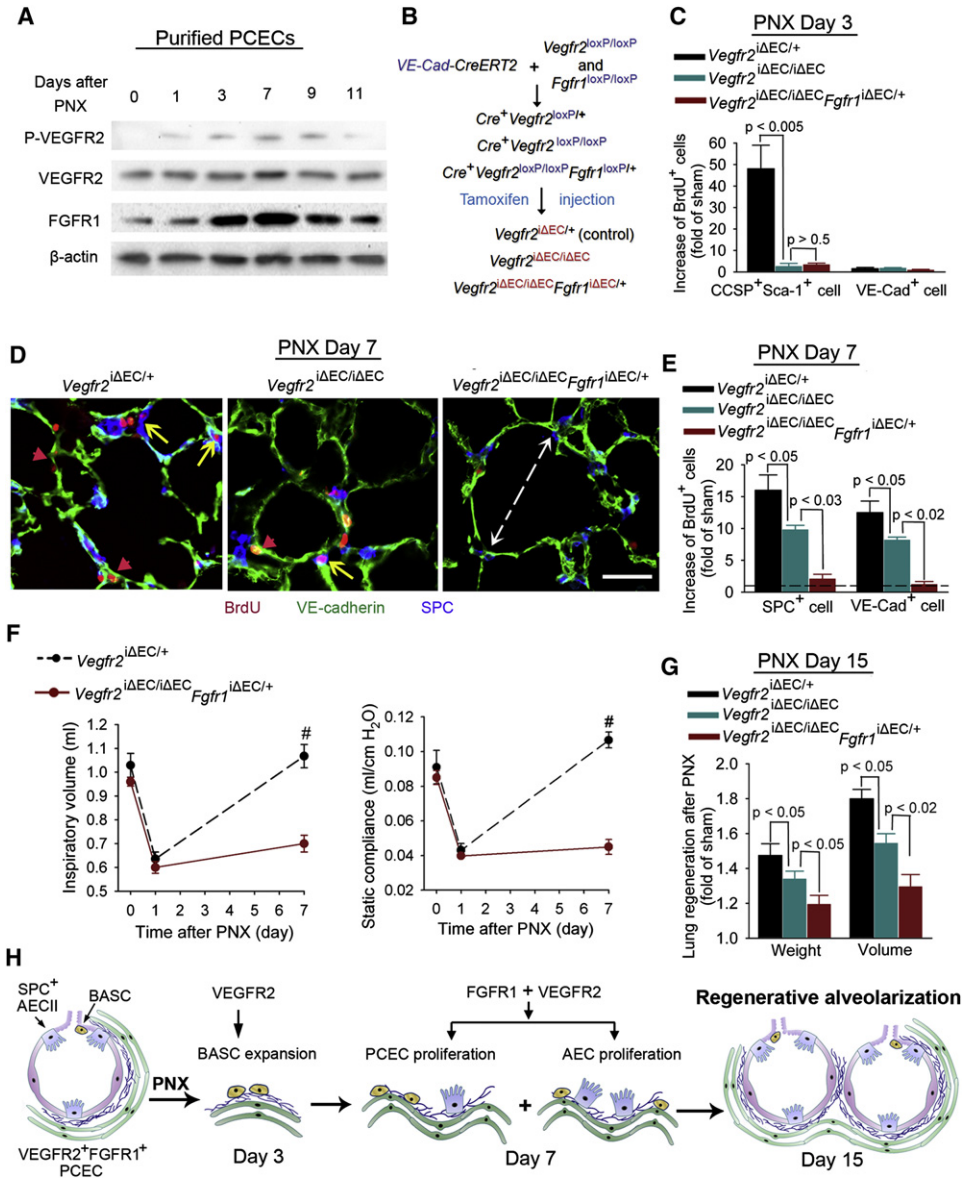

Figure 3. Inducible Deletion of *Vegfr2* and Partial Knockdown of *Fgfr1* in ECs Attenuates Lung Regeneration

(A) Sequential activation of VEGFR2 and upregulation of FGFR1 in PCECs after PNX. VEGFR2 phosphorylation is increased by PNX, whereas total VEGFR2 expression in PCECs remains constant. In contrast, FGFR1 expression in PCECs is upregulated after PNX in a time-dependent manner.

(B) EC-specific knockout of VEGFR2 and FGFR1 in adult mice. Transgenic mice in which *VE-cadherin* promoter drives expression of tamoxifen-responsive CreERT2 (*VE-Cad-CreERT2* mice) were crossed with $Vegfr2^{loxP/loxP}$ and $Fgfr1^{loxP/loxP}$ mice and treated with tamoxifen to induce EC-specific deletion of *Vegfr2* and *Fgfr1* ($Vegfr2^{i\Delta EC/i\Delta EC}$ and $Vegfr2^{i\Delta EC/i\Delta EC}Fgfr1^{i\Delta EC/+}$ mice).

(C) EC-specific deletion of *Vegfr2* ($Vegfr2^{i\Delta EC/i\Delta EC}$ mice) inhibits the expansion of $CCSP^{+}Sca1^{+}$ BASC-like cells after PNX. $Vegfr2^{i\Delta EC/+}$ mice served as control.

(D and E) Defective proliferation of both PCECs (red arrowheads) and AECs (yellow arrows) in $Vegfr2^{i\Delta EC/i\Delta EC}Fgfr1^{i\Delta EC/+}$ mice after PNX. n = 4. Scale bar, 100 μm. Note the increase in alveolar diameter (dashed arrows) in $Vegfr2^{i\Delta EC/i\Delta EC}Fgfr1^{i\Delta EC/+}$ mice as compared to control $Vegfr2^{i\Delta EC/+}$ mice.

(F) After PNX, EC-specific deletion of *Vegfr2* and *Fgfr1* impaired the recovery of pulmonary function. The restoration of pulmonary function in $Vegfr2^{i\Delta EC/i\Delta EC}Fgfr1^{i\Delta EC/+}$ mice was significantly inhibited compared to control mice. Note the normal pulmonary function of knockout mice before PNX. #p < 0.01, compared to control $Vegfr2^{i\Delta EC/+}$ mice. n = 4.

(G) Restoration of lung mass and volume is impaired in $Vegfr2^{i\Delta EC/i\Delta EC}Fgfr1^{i\Delta EC/+}$ mice. n = 4.

(H) Proposed model of PCEC-mediated regulation of regenerative alveolarization. Activation of VEGFR2 in PCECs instigates the early expansion of BASCs, whereas there is minimal proliferation of PCECs. Subsequent upregulation of FGFR1 along with VEGFR2 activation sustains proliferation of PCECs and AECs that peaks at day 7. PCECs through neovascularization and inducing AEC expansion complete regeneration of the right lungs by day 15 after PNX.

See also Figure S2.

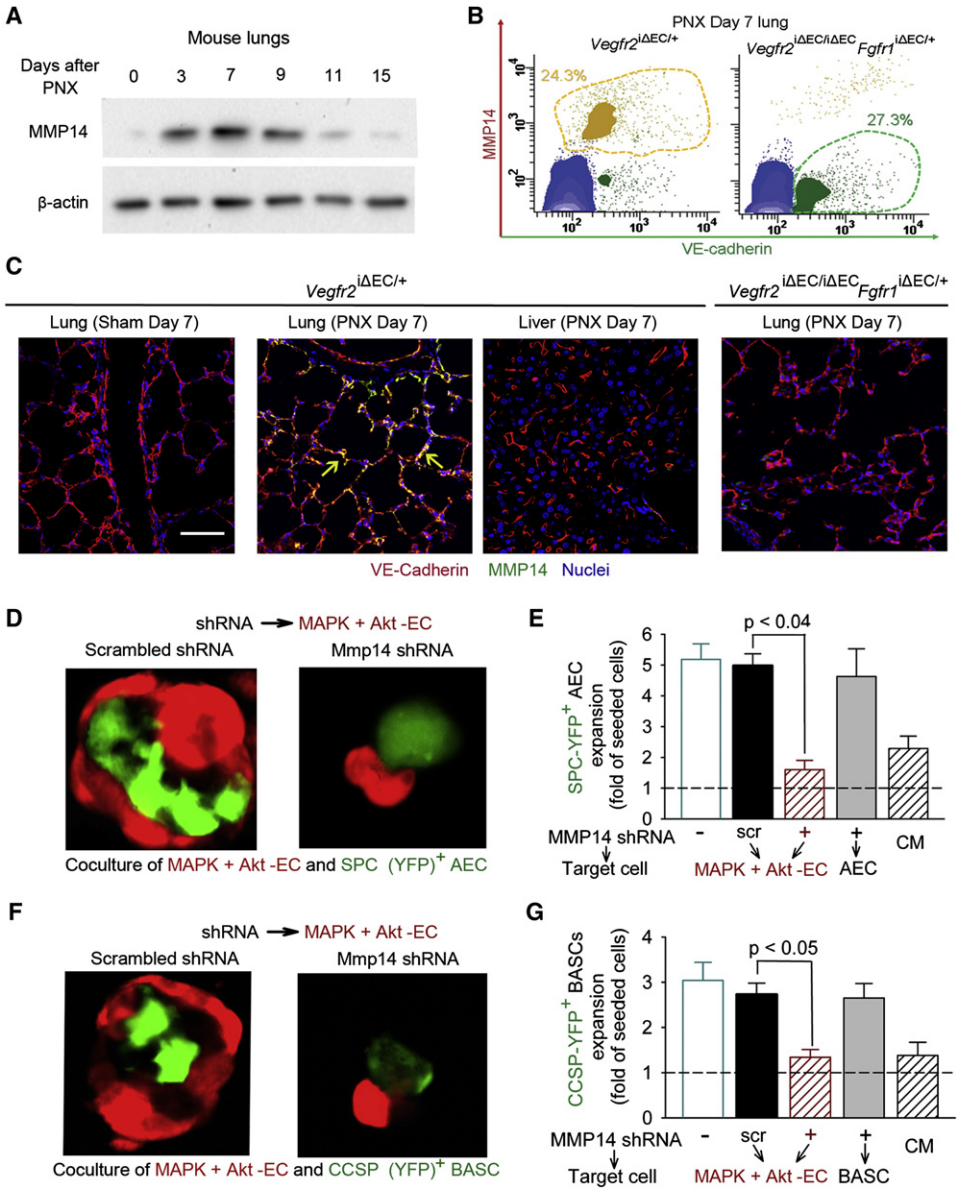

Figure 4. After PNX, MMP14 Is Specifically Produced by PCECs and Induces Formation of Alveolar-Capillary-like Sac in 3D Angiosphere Coculture with Activated ECs

(A) PNX induces time-dependent upregulation of MMP14 protein in the remaining right lobes. Representative western blot image is shown.

(B and C) After PNX, specific upregulation of MMP14 in VE-cadherin$^+$ PCECs is attenuated in *Vegfr2*$^{i\Delta EC/i\Delta EC}$*Fgfr1*$^{i\Delta EC/+}$ mice, as shown by flow cytometry (B) and immunostaining (C). Note the colocalization of upregulated MMP14 in VE-cadherin$^+$ PCECs (arrow), but not liver ECs of pneumonectomized control mice. Scale bar, 100 μm.

(D and E) 3D coculture of SPC (YFP)$^+$ AECIIs with MAPK- and Akt-activated primary ECs (MAPK+Akt ECs) forms angiosphere and establishes a bioreactor for expansion of SPC$^+$ AECs by angiocrine production of MMP14. MAPK+Akt ECs were generated by transducing c-Raf, which activates MAPK pathway, and E4ORF1 gene that sustains Akt co-activation. Representative image (D) and quantification (E) of different groups are shown. scr, scrambled shRNA; CM, conditioned medium.

(F and G) Angiocrine production of MMP14 supports propagation of CCSP (YFP)$^+$Sca-1$^+$CD31$^-$ BASC-like cells. Representative image (F) and quantification (G) of various groups are shown.

See also Figure S3.

in E4ORF1$^+$ ECs (MAPK+Akt ECs) (Kobayashi et al., 2010). Next, MAPK+Akt ECs were cocultured with AECIIs/BASCs in three-dimensional (3D) angiosphere assay. Coculture with MAPK+Akt ECs led to the most significant expansion of SPC$^+$ AECIIs and CCSP$^+$Sca-1$^+$CD31$^-$ BASCs (Figures 4D–4G and S3), resulting in formation of 3D angiospheres, with ECs encircling expanding

epithelial cells, that resemble the structure of an alveolar-capillary sac. MMP14 knockdown in MAPK+Akt ECs abolished expansion of BACSs and AECIIs (Figures 4D and 4F). Conditioned medium (CM) from MAPK+Akt ECs showed a negligible effect in promoting AECII and BASC propagation, underscoring the requirement for cell-cell contact between ECs and epithelial cells (Figures 4E and 4G). Therefore, resection of the left lung activates VEGFR2 and FGFR1 on PCECs triggering MMP14 production, which in turn stimulates propagation of epithelial progenitor cells.

After PNX, MMP14 Inhibition Abrogates the Reconstitution of AECs, but Not PCECs

To determine the physiological significance of MMP14 in modulating alveologenesis, we injected wild-type (WT) mice with a neutralizing monoclonal antibody (mAb) to MMP14. After PNX, the MMP14 mAb attenuated the increase of mass and volume of remaining lungs in WT, but not *Vegfr2*$^{i\Delta EC/i\Delta EC}$*Fgfr1*$^{i\Delta EC/+}$, mice, indicating that MMP14 is derived from VEGFR2- and FGFR1-activated PCECs (Figures 5A and S4). MMP14 inhibition blocked expansion of E-cadherin$^+$ AECs without impairing reconstitution of VE-cadherin$^+$ PCECs (Figure 5B). The mismatched expansion of AECs and PCECs after MMP14 inhibition indicates that MMP14 induces propagation of AECs (inductive angiogenesis), rather than promoting PCEC proliferation (proliferative angiogenesis).

The reduced expansion of AECs, but not PCECs, by MMP14 neutralization was further demonstrated by flow cytometric analysis (Figures 5C and 5D). Furthermore, in mice injected with mAb to MMP14, morphological examination revealed inhibition of alveolar regrowth, as evidenced by a decrease in alveolar number and increase in alveolar size measured by mean alveolar intercept (Figures 5E and 5F). Collagen synthesis remained unchanged in mice injected with mAb to MMP14 (Figure S4). Therefore, PCEC-derived MMP14 stimulates neoalveolarization, forming alveolar sacs reminiscent of normal adult alveoli.

MMP14 Stimulates Alveologenesis via Unmasking of Cryptic EGF-like Ligands

We next sought to unravel the mechanism by which MMP14 regulates regenerative alveolarization. MMP14 has been shown to shed the ectodomain of heparin binding EGF-like growth factor (HB-EGF) (Koshikawa et al., 2010; Stratman et al., 2010). In addition, MMP14 cleaves laminin5 γ2 chain to generate an EGF-like fragment that activates EGF receptor (EGFR) (Schenk et al., 2003). We found that, at days 3 and 7 after PNX, HB-EGF in bronchioalveolar lavage fluid (BALF) is increased (Figures 6A and 6B). The cleaved fragment of laminin5 γ2 chain appeared in regenerating lungs at day 7 after PNX (Figures 6C and S5). However, the level of these EGFR ligands was decreased in both control mice treated with mAb to MMP14 and *Vegfr2*$^{i\Delta EC/i\Delta EC}$*Fgfr1*$^{i\Delta EC/+}$ mice, in which there is diminished expression of MMP14. Knockdown of MMP14 in MAPK+Akt ECs in 3D endothelial coculture with BASCs and AECs also abrogated the release of EGFR ligands to culture supernatant (Figure S5). Hence, after PNX, activation of VEGFR2 and FGFR1 in PCECs leads to angiocrine production of MMP14, which in turn unmasks cryptic EGFR ligands stimulating alveolar regeneration.

EGF Restores Alveolar Epithelialization in *Vegfr2*$^{i\Delta EC/i\Delta EC}$*Fgfr1*$^{i\Delta EC/+}$ Mice

Both shedded HB-EGF and cleaved laminin5 γ2 chain activate EGFR that drives epithelialization. Our findings suggest that, after PNX, impaired lung alveolarization in *Vegfr2*$^{i\Delta EC/i\Delta EC}$ *Fgfr1*$^{i\Delta EC/+}$ mice is due to a decrease in bioavailability of EGFR ligands, implicating that injection of EGF might restore alveolarization in *Vegfr2*$^{i\Delta EC/i\Delta EC}$*Fgfr1*$^{i\Delta EC/+}$ mice by enhancing epithelialization. Intravenous injection of recombinant EGF restored lung mass and volume in *Vegfr2*$^{i\Delta EC/i\Delta EC}$*Fgfr1*$^{i\Delta EC/+}$ mice and mice treated with mAb to MMP14 (Figures 6D and S5). Direct introduction of EGF to bronchioalveolar epithelium via intratracheal injection showed a similar effect in rescuing alveolar regeneration (Figure S5). Therefore, the defective regeneration of AECs in *Vegfr2*$^{i\Delta EC/i\Delta EC}$*Fgfr1*$^{i\Delta EC/+}$ mice (Figure 3) is caused by diminished MMP14 production by PCECs that attenuates bioavailability of EGFR ligands.

Notably, in *Vegfr2*$^{i\Delta EC/i\Delta EC}$*Fgfr1*$^{i\Delta EC/+}$ mice injected with EGF, cellular association of E-cadherin$^+$ AECs with VE-cadherin$^+$ PCECs was enhanced (Figures 6E and S5), restoring pulmonary function (Figure 6F). EGF injection into *Vegfr2*$^{i\Delta EC/i\Delta EC}$*Fgfr1*$^{i\Delta EC/+}$ mice stimulated regeneration of AECs, but not PCECs (Figure S5), suggesting that EGF has a minor effect in triggering angiogenesis while being more effective in driving epithelialization. To test this hypothesis, we analyzed the effect of EGF administration on cell amplification at day 7 after PNX. Injection of EGF led to enhanced EGFR phosphorylation in the *Vegfr2*$^{i\Delta EC/i\Delta EC}$*Fgfr1*$^{i\Delta EC/+}$ lung (Figure 6G). BrdU incorporation analysis revealed that EGF restored proliferation of AECIIs, but not PCECs, in *Vegfr2*$^{i\Delta EC/i\Delta EC}$*Fgfr1*$^{i\Delta EC/+}$ mice (Figures 6H and 6I). Thus, the alveologenic defect in *Vegfr2*$^{i\Delta EC/i\Delta EC}$ *Fgfr1*$^{i\Delta EC/+}$ mice is due to impaired generation of epithelially active angiocrine factors, rather than compromised vascular perfusion to regenerating lung.

Transplantation of Wild-Type PCECs Restores Alveolarization in *Vegfr2*$^{i\Delta EC/i\Delta EC}$*Fgfr1*$^{i\Delta EC/+}$ Mice

In our study, pan-endothelial *VE-cadherin* promoter-driven expression of CreERT2 could delete *Vegfr2* and *Fgfr1* in ECs of other vascular beds. To investigate the specific contribution of activated PCECs to lung regeneration, we designed a lung EC transplantation model. ECs were purified from either lung or liver of pneumonectomized WT littermate mice and were infused into the jugular vein of *Vegfr2*$^{i\Delta EC/i\Delta EC}$ and *Vegfr2*$^{i\Delta EC/i\Delta EC}$*Fgfr1*$^{i\Delta EC/+}$ mice (Figure 7A). Plasma was also collected from pneumonectomized WT mice and injected to recipient knockout mice to interrogate the contribution of systemic soluble growth factors to lung regeneration.

Transplanted GFP$^+$ ECs incorporated into ~26% of pulmonary capillaries of recipient mice (Figures 7B and S6). Importantly, the engrafted ECs obtained from the pneumonectomized lungs, but not the liver, restored the amplification of epithelial cells (Figures 7C–7F and S6). Proliferating BrdU$^+$CCSP$^+$ BASC-like cells and BrdU$^+$SPC$^+$ AECIIs were positioned in the proximity of the transplanted GFP$^+$ PCECs, indicating that inductive signals derived

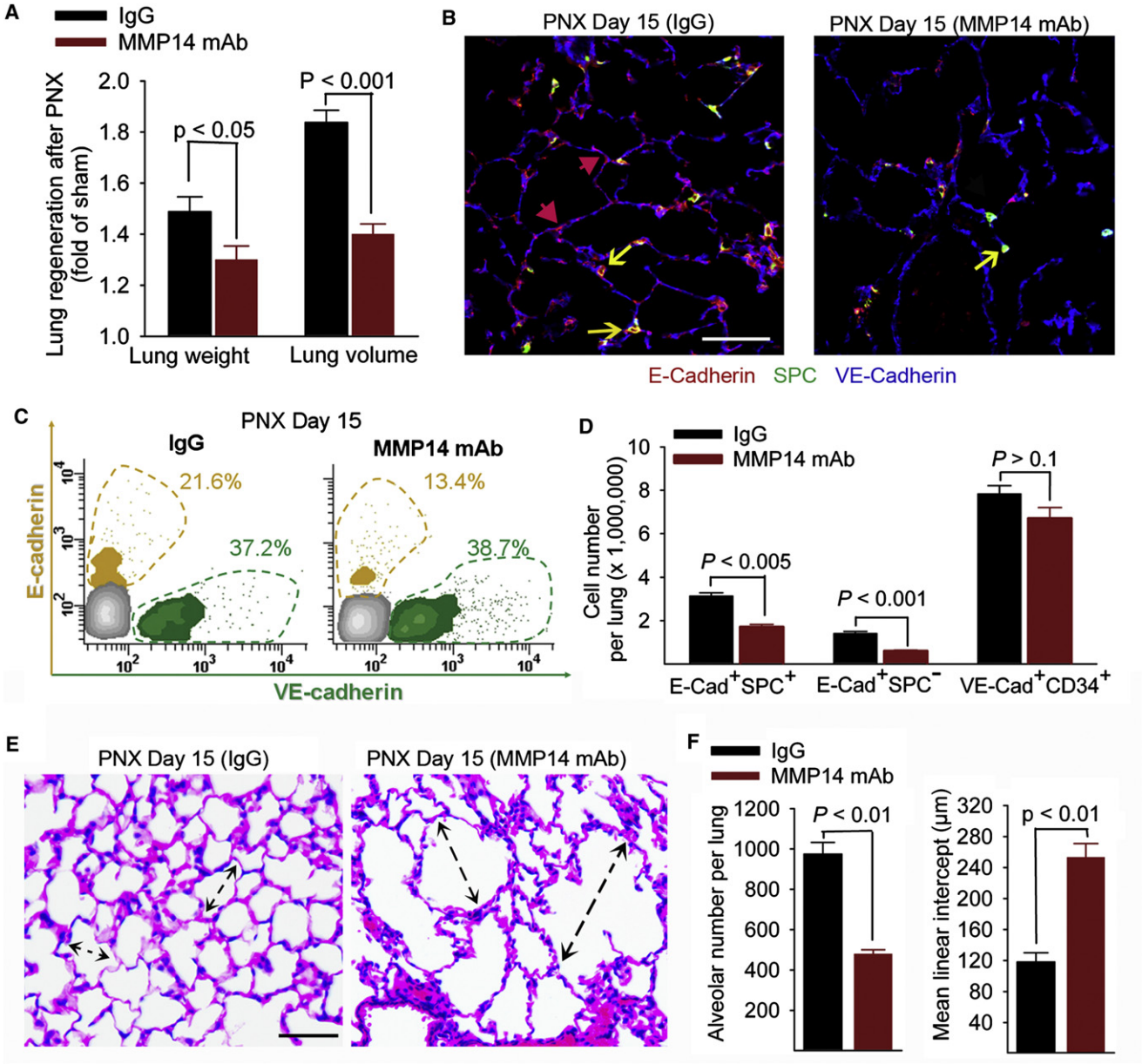

Figure 5. PCEC-Derived MMP14 Supports Regenerative Alveolarization

(A) After PNX, neutralizing mAb to MMP14 abolished regeneration of lung mass and volume.

(B) After PNX, inhibition of MMP14 diminished expansion of E-cadherin$^+$ AECs. n = 5. Scale bar, 100 μm. Note the lack of both cuboidal SPC$^+$E-cadherin$^+$ AECIIs (yellow arrow) and squamous SPC$^-$E-cadherin$^+$ type I-like AECs (red arrowhead) in the alveoli treated with MMP14 mAb.

(C and D) After PNX, MMP14 inhibition blocked expansion of E-cadherin$^+$ AECs, but not VE-cadherin$^+$CD34$^+$ PCECs. n = 5.

(E and F) After PNX, inhibition of MMP14 suppressed alveolar regrowth and led to enlarged alveolar size. (E) Representative hematoxylin and eosin staining of the pneumonectomized lungs treated with neutralizing mAb to MMP14 and isotype IgG. Note the increase in alveolar size in the mAb-treated mice (dashed lines). (F) Quantification of alveolar number and alveolar size after PNX. Scale bar, 100 um.

See also Figure S4.

from the infused WT PCECs restore lung regeneration. Accordingly, pulmonary function was improved by transplantation of PCECs, but not injection of plasma procured from pneumonectomized WT mice (Figure 7G). Therefore, PNX induces a lung-specific activation of PCECs to elaborate angiocrine factors that support regenerative lung alveolarization (Figure 7H).

DISCUSSION

After PNX, Activation of PCECs Supports Expansion of Epithelial Progenitor Cells

We have employed a PNX-induced alveolar regeneration model, endothelial-specific knockdown of *Vegfr2* and *Fgfr1*, and 3D

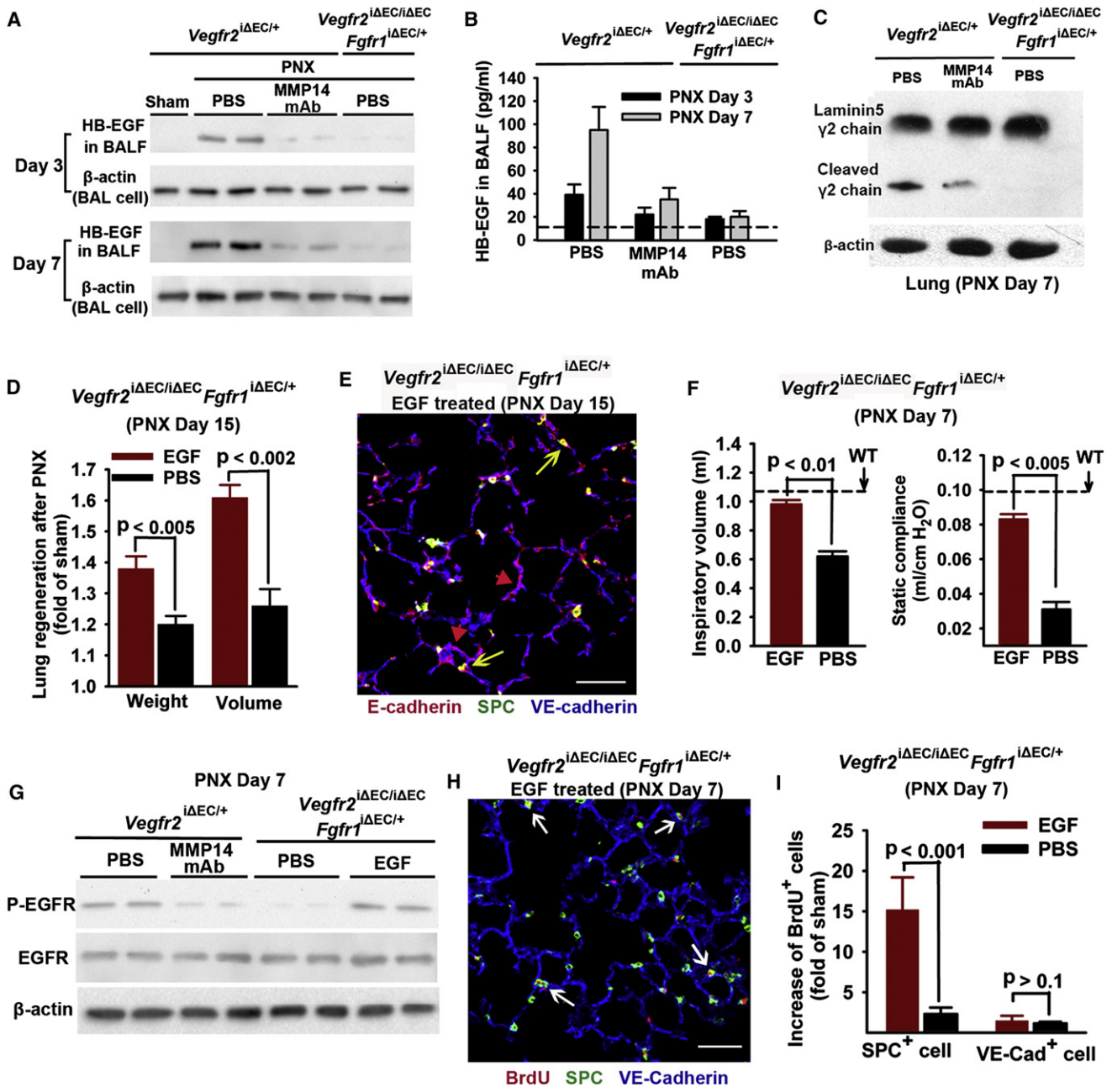

Figure 6. Angiocrine Production of MMP14 Induces Alveologenesis by Shedding EGF-like Ectodomains from HB-EGF and Laminin5 γ2 Chain

(A and B) PNX induced time-dependent release of HB-EGF into alveolar space, which is inhibited in *Vegfr2*$^{i\Delta EC/i\Delta EC}$*Fgfr1*$^{i\Delta EC/+}$ mice or by MMP14 neutralization. Representative western blot image is shown in (A). Control *Vegfr2*$^{i\Delta EC/+}$ mice treated with neutralizing mAb to MMP14 (MMP14 mAb). BAL, bronchioalveolar lavage; BALF, BAL fluid. n = 4.

(C) At day 7 after PNX, activation of VEGFR2 and FGFR1 in PCECs upregulated MMP14, causing cleavage of laminin5 γ2 chain.

(D–F) EGF injection restored: (1) regeneration of lung mass and volume (D), (2) integration of E-cadherin$^+$ AECs within the capillary (E), and (3) pulmonary function measured by inspiratory volume and static compliance (F) in *Vegfr2*$^{i\Delta EC/i\Delta EC}$*Fgfr1*$^{i\Delta EC/+}$ mice after PNX. Note the enhanced association of SPC$^-$E-cadherin$^+$ AECIIs (red arrowhead) and SPC$^+$E-cadherin$^+$ AECIIs (yellow arrow) with the capillary. n = 4.

(G–I) At day 7 after PNX, intravenous EGF injection restored EGFR phosphorylation (G) and increased proliferation of SPC$^+$ AECIIs (H and I) in the *Vegfr2*$^{i\Delta EC/i\Delta EC}$*Fgfr1*$^{i\Delta EC/+}$ lung. Note the augmented proliferation in SPC$^+$ AECIIs (white arrow). Quantification of amplifying cell population after PNX is shown in (I). n = 4. Scale bar, 100 μm.

See also Figure S5.

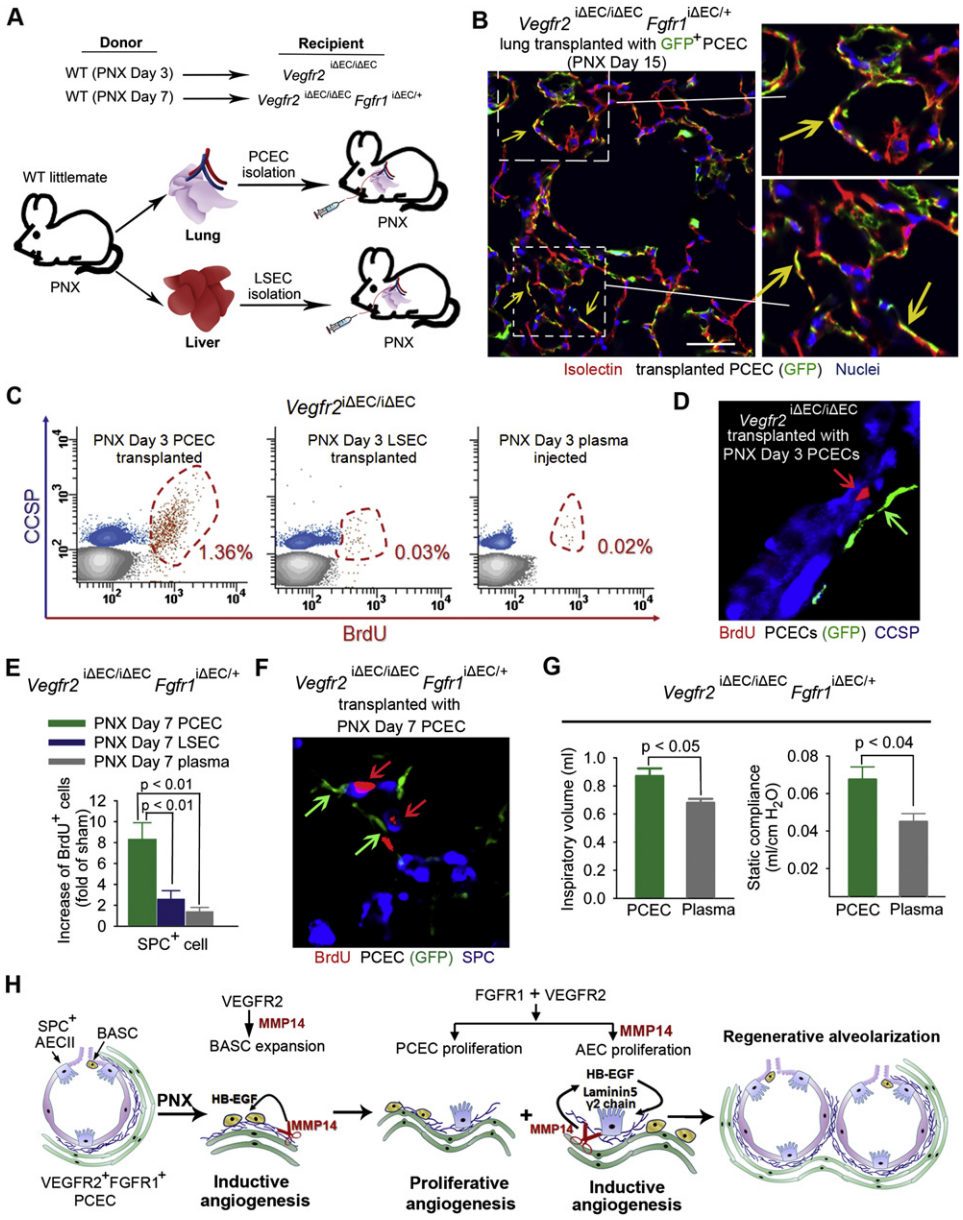

Figure 7. Transplantation of Wild-Type PCECs Restores Defective Alveolar Regeneration in Mice Deficient in Endothelial *Vegfr2* and *Fgfr1*

(A) EC transplantation strategy to define contribution of PCECs in promoting alveolar regeneration. After PNX, ECs were purified from the lung and liver of WT littermates, transduced with lentiviral GFP, and transplanted via the jugular vein into pneumonectomized *Vegfr2*$^{i\Delta EC/i\Delta EC}$ and *Vegfr2*$^{i\Delta EC/i\Delta EC}$*Fgfr1*$^{i\Delta EC/+}$ mice at days 3 and 7, respectively.

(B) Incorporation of transplanted GFP$^+$ PCECs into functional lung capillary. Intravenous infusion of vascular-specific isolectin was used to identify patent vasculature. Note the presence of perfused isolectin$^+$GFP$^+$ PCECs, indicating functional incorporation of transplanted WT PCECs into recipient *Vegfr2*$^{i\Delta EC/i\Delta EC}$*Fgfr1*$^{i\Delta EC/+}$ capillaries. Scale bar, 100 μm.

(C and D) Restoration of expansion potential of CCSP$^+$ BASC-like cells in *Vegfr2*$^{i\Delta EC/i\Delta EC}$ mice after PCEC transplantation. Note in (D) the unique localization of proliferating BrdU$^+$CCSP$^+$ BASC-like cells (red arrow) that is in close proximity to transplanted GFP$^+$ PCECs (green arrow).

(E–G) Transplantation of WT PCECs restores proliferation of SPC$^+$ AECs (E and F) and pulmonary function (G) in *Vegfr2*$^{i\Delta EC/i\Delta EC}$*Fgfr1*$^{i\Delta EC/+}$ mice. Expanding BrdU$^+$SPC$^+$ AECs (red arrow) were detected in close cellular association with transplanted PCECs (green arrow) (F).

(H) Proposed model illustrating the inductive role of VEGFR2- and FGFR1-primed PCECs in lung regenerative alveolarization. Upon PNX, activation of VEGFR2 in PCECs leads to MMP14 production and HB-EGF release to stimulate the expansion of epithelial progenitor cells (BASCs and AECIIs). Subsequent activation of FGFR1 along with VEGFR2 stimulates proliferation of PCECs maintaining MMP14 expression. MMP14 unmasks cryptic EGFR ligands through shedding of HB-EGF and cleaving laminin5 γ2 chain, which by activating EGFR, induces proliferation of SPC$^+$E-cadherin$^+$ AECs. After PNX, sequential propagation of epithelial cells induced by PCEC-derived MMP14 and increase in bioavailability of EGFR-ligands culminate in full reconstitution of functional alveolar-capillary sacs. Proliferation of PCECs vascularizes the regenerating lung tissue to restore the blood supply and gas exchange function.

See also Figure S6.

endothelial-epithelial coculture angiosphere bioreactors to establish the essential role of the PCECs in promoting regenerative alveologenesis. We have uncovered the angiocrine role of MMP14, which by shedding HB-EGF and generating an EGF-like fragment from laminin5 γ2 chain, stimulates amplification of lung epithelial progenitor cells, including subsets of BASCs and AECs, supporting alveolarization. The role of MMP14/EGFR activation in promoting alveologenesis was borne out in studies in which EGF administration into *Vegfr2*$^{i\Delta EC/i\Delta EC}$ *Fgfr1*$^{i\Delta EC/+}$ mice restored alveolar regeneration after PNX. Moreover, we established a lung PCEC transplantation model to define the essential role of functionally incorporated PCECs in restoring epithelialization in mice with impaired capacity to undergo neoalveolarization. Taken together, we have demonstrated that, after PNX, PCECs orchestrate regenerative alveolarization by formation of new vessels and through instructive production of epithelial-active angiocrine factors.

PNX induced alveolar regeneration via amplification of epithelial progenitor cells. At early phases (day 0–3), PNX induces expansion of CCSP$^+$SPC$^+$Sca-1$^+$CD31$^-$VE-cadherin$^-$ BASC-like cells localized at BADJ. At later phases (day 7–15), SPC$^+$E-cadherin$^+$ AECIIs and PCECs expand, reestablishing functional alveolar-capillary units. Upon MMP14 inhibition, loss of alveolar coverage of not only cuboidal SPC$^+$E-cadherin$^+$, but also squamous SPC$^-$E-cadherin$^+$ AEC, implicates that transiently amplified SPC$^+$E-cadherin$^+$ AECIIs potentially generate SPC$^-$E-cadherin$^+$ type I AECs (Beers and Morrisey, 2011; Morrisey and Hogan, 2010; Rock and Hogan, 2011), leading to full reconstitution of alveolar surface after PNX. Therefore, activated PCECs drive regeneration of specialized lung epithelial cells that collectively rebuild functional alveolar-capillary sacs.

PCECs Initiate Alveologenesis through MMP14-Mediated Release of EGFR Ligands

We show that PCEC-derived MMP14 is required for the expansion of epithelial cells and restoration of alveolar structure and pulmonary function. In mouse fetal lung, MMP14 regulates alveolar formation (Atkinson et al., 2005; Irie et al., 2005; Oblander et al., 2005; Greenlee et al., 2007) by provoking epithelial proliferation and migration (Chun et al., 2006; Hiraoka et al., 1998; Stratman et al., 2009; Yana et al., 2007). Postnatally, MMP14-deficient mice exhibit defective alveolarization, abnormal sacculation, and impaired vascular integration with AECs, suggesting that MMP14 mediates alveolar-capillary crosstalk (Lee et al., 2004; Li et al., 2002; Morris et al., 2003; Page-McCaw et al., 2007). Here, we show that, after PNX, inhibition of MMP14 interfered with alveolar regrowth, but not endothelial proliferation, leading to enlarged alveolar size. This suggests that MMP14 is dispensable for proliferative angiogenesis but plays a key role in inducing regenerative alveolarization. The mechanism by which MMP14 modulates alveologenesis involves shedding of HB-EGF into the alveolar space and generation of an EGF-like fragment from laminin5 γ2 chain. Subsequently, an increase in bioavailable EGFR ligands initiates regeneration of epithelial progenitors. In this regard, MMP14 performs as a PCEC-specific angiocrine cue that drives regenerative alveolarization.

PCEC-Specific Induction of MMP14 Defines Unique Functional Signature of Lung Vasculature

Each organ is vascularized by specialized populations of capillary ECs identified by unique phenotypic, functional, and structural attributes. We have shown that bone marrow (Butler et al., 2010b; Hooper et al., 2009) and liver (Ding et al., 2010) SECs, which are demarcated by VEGFR2$^+$VEGFR3$^+$ VE-cadherin$^+$ vessels, express a defined set of angiocrine factors driving organ regeneration. After partial hepatectomy, VEGFR2- and Id1-activated liver SECs produce HGF and WNT2 (Ding et al., 2010), whereas bone marrow VEGFR2-activated SECs express Notch ligands and IGFBPs (Butler et al., 2010b; Kobayashi et al., 2010) to induce reconstitution of hepatocytes and hematopoietic cells, respectively.

Similarly, PCECs have a distinct phenotypic signature identified as VEGFR2$^+$FGFR1$^+$CD34$^+$VE-cadherin$^+$ vessels. Remarkably, after PNX, the production of MMP14 is restricted to VEGFR2- and FGFR1-activated PCECs, but not other vascular-rich organs, highlighting a unique functional signature of PCECs in alveolar regeneration. The negligible effect of plasma obtained from pneumonectomized WT mice in restoring alveologenesis demonstrated the minimal contribution of systemic soluble growth factor(s) from nonpulmonary vasculature in mediating alveologenesis. These data clearly set forth the notion that PNX turns on a PCEC-specific program to promote alveolar regeneration.

The mechanism by which PNX specifically upregulates MMP14 in PCECs could be regulated by microenvironmental cues and/or unique inherent programming of PCECs. For example, surgical removal of left lung leads to activation of PCECs in the remaining right lungs, without affecting other vascular beds (Figure 1A). Alternatively, PCECs, but not other organ-specific capillaries, may be developmentally predetermined to express MMP14 in response to regenerative signals. Notwithstanding the potential developmental or microenvironmental cues that endow PCECs with their unique functional attributes, our findings consolidate the concept that angiocrine heterogeneity plays a key role in orchestrating organ regeneration.

Sequential Activation of VEGFR2 and FGFR1 Primes PCECs during Alveolar Regeneration

The mechanism by which PCECs are induced to express MMP14 after PNX is mediated by hierarchical activation and upregulation of VEGFR2 and FGFR1. At the early phase of PNX, expansion of BASC-like cells is largely dependent on activation of VEGFR2 in PCECs, which causes upregulation of MMP14 without inducing EC proliferation. In contrast to early activation and stable expression of VEGFR2 after PNX, FGFR1 expression level is induced thereafter, peaking at day 7. We show that FGFR1 synergizes with VEGFR2 in augmenting MMP14 generation, thereby sustaining alveolar regeneration. Sequential activation of VEGFR2 and FGFR1 in PCECs therefore induces MMP14 production, fostering regeneration of the functional alveolar-capillary units.

PCEC Transplantation and Administration of PCEC-Derived Angiocrine Factors Offer Approaches for Treatment of Respiratory Diseases

Development of therapeutic strategies to repair respiratory capacity in patients with pulmonary disorders is handicapped

by a lack of understanding of lung regeneration mechanisms (Jiang et al., 2005; Kajstura et al., 2011; Matthay and Zemans, 2011; Morris et al., 2003; Petrache et al., 2005; Whitsett et al., 2010). We have set forth the concept that, after PNX, activated PCECs play a seminal role in restoring respiratory capacity, as measured by inspiratory volume and static compliance. Notably, administration of EGF or transplantation of activated PCECs improved respiratory function in mice. It is plausible that transplantation of properly activated PCECs or injection of lung-specific angiocrine mediators could improve lung function in subsets of patients with pulmonary disorders.

In conclusion, we have introduced the concept that PCECs not only form passive vascular conduits to fulfill the metabolic demands of regenerating lungs, but also, by relaying inductive angiocrine growth signals such as MMP14, orchestrate regenerative alveologenesis. Selective activation of VEGFR2 and FGFR1 or increase in the production of MMP14, as well as other as yet unrecognized angiocrine factors in PCECs, might facilitate lung alveolarization, thereby improving hypoxemia in patients with debilitating lung diseases.

EXPERIMENTAL PROCEDURES

Transgenic Reporter and Gene-Targeted Animals

Generation of endothelial-specific *Vegfr2*- and *Fgfr1*-inducible knockout mice was carried out as described (Hooper et al., 2009; Wang et al., 2010). In brief, *Vegfr2*$^{loxP/loxP}$ and *Fgfr1*$^{loxP/loxP}$ mice were bred with *VE-cadherin-CreERT2* transgenic mice to establish *VE-cadherin-CreERT2*$^{+}$*Vegfr2*$^{LoxP/LoxP}$ and *VE-cadherin-CreERT2*$^{+}$*Vegfr2*$^{loxP/loxP}$*Fgfr1*$^{loxP/+}$ mice. These mice were treated i.p. with tamoxifen, leading to endothelial-specific deletion of *Vegfr2* and *Fgfr1*.

Mice bearing *SPC* and *CCSP* promoter-driven rtTA (*SPC-rtTA* and *CCSP-rtTA*) and (tetO)7CMV-driven cre ((*tetO*)$_7$*-cre*) (Perl et al., 2002) were crossed with Rosa26R-eYFP mice as described (Rawlins et al., 2009), resulting in *SPC-YFP* and *CCSP-YFP* reporter mice upon tetracycline treatment. All experiments were carried out under guidelines set by Institutional Animal Care and Use Committee.

PNX Model and Physiological Measurements of Lung Mechanics

PNX procedure was adapted as described (Nolen-Walston et al., 2008). In brief, orotracheal intubation was performed in anesthetized and mechanically ventilated mice. Left lung lobe was lifted with a suture tied around the hilum and resected. Sham mice underwent thoracotomy without lobe resection. Lung mass and volume were measured and normalized to body weight after PNX. Isolation of PCECs and examination of phosphorylation and protein level of VEGFR2 and FGFR1 was carried out as described (Ding et al., 2010; Murakami et al., 2011). Inspiratory capacity was determined between the plateau pressure measurements of the lung capacity (TLC) and functional residual volume (FRC) using the Flexivent software (Scireq). Static compliance was determined from pressure-volume curves.

Immunofluorescence and Flow Cytometric Analysis

To perform immunofluorescence (IF) studies, cryopreserved sections were incubated in antibodies recognizing VE-cadherin (R&D), CD34 (BD), E-cadherin (eBiosciences), and SPC (Abcam) and fluorophore-conjugated second antibodies (Jackson Immuno Research). Transit cell amplification was measured by BrdU uptake (Ding et al., 2010). To track proliferating BASC-like cells, BrdU was introduced in drinking water (Nolen-Walston et al., 2008). Images were captured on AxioVert LSM710 microscope (Zeiss). Morphological analysis of alveolar number and mean linear intercept was performed (DeLisser et al., 2006). Total lung cells were isolated and analyzed on LSRII-SORP (BD) (Ding et al., 2010). AECs and PCECs were quantified by staining with conjugated antibodies against SPC+E-cadherin and VE-cadherin+CD34, respectively.

Pharmacological Administration of EGF and Neutralizing mAb to MMP14

Mice were injected with mAb to mouse MMP14 (MMP14 mAb, 50 mg/kg, Abcam) and IgG control 12 hr before PNX and every other day. To determine the role of recombinant EGF in alveolar regeneration, mice were i.v. injected with 500 μg/kg EGF (Abcam) on a daily basis after PNX. Mice were also intratracheally injected with 100 μg/kg EGF (in 50 μl) every other day to test the local effect of EGF.

Determination of AECII and BASC Proliferation in Coculture with Primary ECs

To maintain Akt activation, primary ECs were transduced with E4ORF1 gene (Seandel et al., 2008). To coactivate MAPKinase pathway, c-Raf was introduced in primary E4ORF1^{+} ECs. The resultant MAPK+Akt ECs (Kobayashi et al., 2010) were cocultured with AECIIs and BASCs isolated from *SPC* and *CCSP-YFP* mice (Kim et al., 2005). *Mmp14* or scrambled shRNA was used to knock down *Mmp14* in MAPK+Akt ECs or AECs (Ding et al., 2010). For coculture studies, isolated SPC^{+} AECIIs and BASCs were plated in nonadherent dish seeded with 10-fold more MAPK+Akt ECs. Conditioned medium from MAPK+Akt ECs was added to AECs. After coculture, AECIIs and BASCs were quantified by flow cytometric analysis.

qPCR, ELISA, and Immunoblot Analyses

After PNX, total RNA was isolated from the mouse lungs to perform qPCR using Taqman expression systems (Applied Biosystems). HB-EGF concentration in BALF was examined by sandwich ELISA and western blot using anti-HB-EGF antibodies (Santa Cruz), and cleavage of laminin5 γ2 chain was tested with antibody against γ2 chain (Santa Cruz).

Data Analysis

All data are presented as mean ± SEM. Differences between groups were tested for statistical significance using Student's t test or analysis of variance (ANOVA). Statistical significance was set at $p < 0.05$.

SUPPLEMENTAL INFORMATION

Supplemental Information includes six figures and one table and can be found with this article online at doi:10.1016/j.cell.2011.10.003.

ACKNOWLEDGMENTS

B.-S.D. is a Druckenmiller Fellow of New York Stem Cell Foundation. S.R. is supported by Ansary Stem Cell Institute; Howard Hughes Medical Institute; Empire State Stem Cell Board and New York State Department of Health grants (NYSTEM, C024180, C026438, C026878); National Heart Lung and Blood Institute; Qatar National Priorities Research Foundation NPRP08-663-3-140; and Anbinder and Newmans Own Foundation. T.N.S. is supported by Takeda Science Foundation, Uehara Memorial Foundation, JSPS (Kiban S). M.S. is supported by R01HL53793. *VE-Cad-CreERT2* mice were gift from Dr. Ralf H. Adams (Max Planck Institute). *SPC/CCSP-rtTA* and (*tetO*)*-cre* mice were provided by Drs. Jeffrey A. Whitsett and Anne-Karina T. Perl (Cincinnati Children's Hospital Medical Centre). *Fgfr1*$^{loxP/loxP}$ mice were offered by Drs. Michael Simons and Masahiro Murakami (Yale University). The authors are grateful to Ms. Biin Sung for assistance in lung mechanics measurement.

Received: May 10, 2011
Revised: August 15, 2011
Accepted: October 5, 2011
Published: October 27, 2011

REFERENCES

Aird, W.C. (2007). Phenotypic heterogeneity of the endothelium: I. Structure, function, and mechanisms. Circ. Res. *100*, 158–173.

Alvarez, D.F., Huang, L., King, J.A., ElZarrad, M.K., Yoder, M.C., and Stevens, T. (2008). Lung microvascular endothelium is enriched with progenitor cells that exhibit vasculogenic capacity. Am. J. Physiol. Lung Cell. Mol. Physiol. *294*, L419–L430.

Atkinson, J.J., Holmbeck, K., Yamada, S., Birkedal-Hansen, H., Parks, W.C., and Senior, R.M. (2005). Membrane-type 1 matrix metalloproteinase is required for normal alveolar development. Dev. Dyn. *232*, 1079–1090.

Beers, M.F., Kim, C.Y., Dodia, C., and Fisher, A.B. (1994). Localization, synthesis, and processing of surfactant protein SP-C in rat lung analyzed by epitope-specific antipeptide antibodies. J. Biol. Chem. *269*, 20318–20328.

Beers, M.F., and Morrisey, E.E. (2011). The three R's of lung health and disease: repair, remodeling, and regeneration. J. Clin. Invest. *121*, 2065–2073.

Bhattacharya, J. (2005). Alveolocapillary cross-talk: Giles F. Filley lecture. Chest ***128***(6, Suppl), 553S–555S.

Butler, J.M., Kobayashi, H., and Rafii, S. (2010a). Instructive role of the vascular niche in promoting tumour growth and tissue repair by angiocrine factors. Nat. Rev. Cancer *10*, 138–146.

Butler, J.M., Nolan, D.J., Vertes, E.L., Varnum-Finney, B., Kobayashi, H., Hooper, A.T., Seandel, M., Shido, K., White, I.A., Kobayashi, M., et al. (2010b). Endothelial cells are essential for the self-renewal and repopulation of Notch-dependent hematopoietic stem cells. Cell Stem Cell *6*, 251–264.

Cardoso, W.V. (2001). Molecular regulation of lung development. Annu. Rev. Physiol. *63*, 471–494.

Carmeliet, P. (2005). Angiogenesis in life, disease and medicine. Nature *438*, 932–936.

Chapman, H.A. (2011). Epithelial-mesenchymal interactions in pulmonary fibrosis. Annu. Rev. Physiol. *73*, 413–435.

Chapman, H.A., Li, X., Alexander, J.P., Brumwell, A., Lorizio, W., Tan, K., Sonnenberg, A., Wei, Y., and Vu, T.H. (2011). Integrin $\alpha 6\beta 4$ identifies an adult distal lung epithelial population with regenerative potential in mice. J. Clin. Invest. *121*, 2855–2862.

Chun, T.H., Hotary, K.B., Sabeh, F., Saltiel, A.R., Allen, E.D., and Weiss, S.J. (2006). A pericellular collagenase directs the 3-dimensional development of white adipose tissue. Cell *125*, 577–591.

Cowan, M.J., and Crystal, R.G. (1975). Lung growth after unilateral pneumonectomy: quantitation of collagen synthesis and content. Am. Rev. Respir. Dis. *111*, 267–277.

Del Moral, P.M., Sala, F.G., Tefft, D., Shi, W., Keshet, E., Bellusci, S., and Warburton, D. (2006). VEGF-A signaling through Flk-1 is a critical facilitator of early embryonic lung epithelial to endothelial crosstalk and branching morphogenesis. Dev. Biol. *290*, 177–188.

DeLisser, H.M., Helmke, B.P., Cao, G., Egan, P.M., Taichman, D., Fehrenbach, M., Zaman, A., Cui, Z., Mohan, G.S., Baldwin, H.S., et al. (2006). Loss of PECAM-1 function impairs alveolarization. J. Biol. Chem. *281*, 8724–8731.

Ding, B.S., Nolan, D.J., Butler, J.M., James, D., Babazadeh, A.O., Rosenwaks, Z., Mittal, V., Kobayashi, H., Shido, K., Lyden, D., et al. (2010). Inductive angiocrine signals from sinusoidal endothelium are required for liver regeneration. Nature *468*, 310–315.

Giordano, R.J., Lahdenranta, J., Zhen, L., Chukwueke, U., Petrache, I., Langley, R.R., Fidler, I.J., Pasqualini, R., Tuder, R.M., and Arap, W. (2008). Targeted induction of lung endothelial cell apoptosis causes emphysema-like changes in the mouse. J. Biol. Chem. *283*, 29447–29460.

Greenlee, K.J., Werb, Z., and Kheradmand, F. (2007). Matrix metalloproteinases in lung: multiple, multifarious, and multifaceted. Physiol. Rev. *87*, 69–98.

Hiraoka, N., Allen, E., Apel, I.J., Gyetko, M.R., and Weiss, S.J. (1998). Matrix metalloproteinases regulate neovascularization by acting as pericellular fibrinolysins. Cell *95*, 365–377.

Hooper, A.T., Butler, J.M., Nolan, D.J., Kranz, A., Iida, K., Kobayashi, M., Kopp, H.G., Shido, K., Petit, I., Yanger, K., et al. (2009). Engraftment and reconstitution of hematopoiesis is dependent on VEGFR2-mediated regeneration of sinusoidal endothelial cells. Cell Stem Cell *4*, 263–274.

Huh, D., Matthews, B.D., Mammoto, A., Montoya-Zavala, M., Hsin, H.Y., and Ingber, D.E. (2010). Reconstituting organ-level lung functions on a chip. Science *328*, 1662–1668.

Irie, K., Komori, K., Seiki, M., Tsuruga, E., Sakakura, Y., Kaku, T., and Yajima, T. (2005). Impaired alveolization in mice deficient in membrane-type matrix metalloproteinase 1 (MT1-MMP). Med. Mol. Morphol. *38*, 43–46.

Jiang, D., Liang, J., Fan, J., Yu, S., Chen, S., Luo, Y., Prestwich, G.D., Mascarenhas, M.M., Garg, H.G., Quinn, D.A., et al. (2005). Regulation of lung injury and repair by Toll-like receptors and hyaluronan. Nat. Med. *11*, 1173–1179.

Kajstura, J., Rota, M., Hall, S.R., Hosoda, T., D'Amario, D., Sanada, F., Zheng, H., Ogórek, B., Rondon-Clavo, C., Ferreira-Martins, J., et al. (2011). Evidence for human lung stem cells. N. Engl. J. Med. *364*, 1795–1806.

Kim, C.F., Jackson, E.L., Woolfenden, A.E., Lawrence, S., Babar, I., Vogel, S., Crowley, D., Bronson, R.T., and Jacks, T. (2005). Identification of bronchioalveolar stem cells in normal lung and lung cancer. Cell *121*, 823–835.

Kobayashi, H., Butler, J.M., O'Donnell, R., Kobayashi, M., Ding, B.S., Bonner, B., Chiu, V.K., Nolan, D.J., Shido, K., Benjamin, L., and Rafii, S. (2010). Angiocrine factors from Akt-activated endothelial cells balance self-renewal and differentiation of haematopoietic stem cells. Nat. Cell Biol. *12*, 1046–1056.

Komarova, Y., and Malik, A.B. (2010). Regulation of endothelial permeability via paracellular and transcellular transport pathways. Annu. Rev. Physiol. *72*, 463–493.

Koshikawa, N., Mizushima, H., Minegishi, T., Iwamoto, R., Mekada, E., and Seiki, M. (2010). Membrane type 1-matrix metalloproteinase cleaves off the NH2-terminal portion of heparin-binding epidermal growth factor and converts it into a heparin-independent growth factor. Cancer Res. *70*, 6093–6103.

Kotton, D.N., and Fine, A. (2008). Lung stem cells. Cell Tissue Res. *331*, 145–156.

Lammert, E., Cleaver, O., and Melton, D. (2001). Induction of pancreatic differentiation by signals from blood vessels. Science *294*, 564–567.

Lee, C.G., Link, H., Baluk, P., Homer, R.J., Chapoval, S., Bhandari, V., Kang, M.J., Cohn, L., Kim, Y.K., McDonald, D.M., and Elias, J.A. (2004). Vascular endothelial growth factor (VEGF) induces remodeling and enhances TH2-mediated sensitization and inflammation in the lung. Nat. Med. *10*, 1095–1103.

Leuwerke, S.M., Kaza, A.K., Tribble, C.G., Kron, I.L., and Laubach, V.E. (2002). Inhibition of compensatory lung growth in endothelial nitric oxide synthase-deficient mice. Am. J. Physiol. Lung Cell. Mol. Physiol. *282*, L1272–L1278.

Li, Q., Park, P.W., Wilson, C.L., and Parks, W.C. (2002). Matrilysin shedding of syndecan-1 regulates chemokine mobilization and transepithelial efflux of neutrophils in acute lung injury. Cell *111*, 635–646.

Liu, Y., Sadikot, R.T., Adami, G.R., Kalinichenko, V.V., Pendyala, S., Natarajan, V., Zhao, Y.Y., and Malik, A.B. (2011). FoxM1 mediates the progenitor function of type II epithelial cells in repairing alveolar injury induced by Pseudomonas aeruginosa. J. Exp. Med. *208*, 1473–1484.

Matsumoto, K., Yoshitomi, H., Rossant, J., and Karet, K.S. (2001). Liver organogenesis promoted by endothelial cells prior to vascular function. Science *294*, 559–563.

Matthay, M.A., and Zemans, R.L. (2011). The acute respiratory distress syndrome: pathogenesis and treatment. Annu. Rev. Pathol. *6*, 147–163.

Metzger, R.J., Klein, O.D., Martin, G.R., and Krasnow, M.A. (2008). The branching programme of mouse lung development. Nature *453*, 745–750.

Morris, D.G., Huang, X., Kaminski, N., Wang, Y., Shapiro, S.D., Dolganov, G., Glick, A., and Sheppard, D. (2003). Loss of integrin alpha(v)beta6-mediated TGF-beta activation causes Mmp12-dependent emphysema. Nature *422*, 169–173.

Morrisey, E.E., and Hogan, B.L. (2010). Preparing for the first breath: genetic and cellular mechanisms in lung development. Dev. Cell *18*, 8–23.

Murakami, M., Nguyen, L.T., Hatanaka, K., Schachterle, W., Chen, P.Y., Zhuang, Z.W., Black, B.L., and Simons, M. (2011). FGF-dependent regulation of VEGF receptor 2 expression in mice. J. Clin. Invest. *121*, 2668–2678.

Muzykantov, V.R. (2005). Biomedical aspects of targeted delivery of drugs to pulmonary endothelium. Expert Opin. Drug Deliv. *2*, 909–926.

Nolen-Walston, R.D., Kim, C.F., Mazan, M.R., Ingenito, E.P., Gruntman, A.M., Tsai, L., Boston, R., Woolfenden, A.E., Jacks, T., and Hoffman, A.M. (2008). Cellular kinetics and modeling of bronchioalveolar stem cell response during lung regeneration. Am. J. Physiol. Lung Cell. Mol. Physiol. *294*, L1158–L1165.

Oblander, S.A., Zhou, Z., Gálvez, B.G., Starcher, B., Shannon, J.M., Durbeej, M., Arroyo, A.G., Tryggvason, K., and Apte, S.S. (2005). Distinctive functions of membrane type 1 matrix-metalloprotease (MT1-MMP or MMP-14) in lung and submandibular gland development are independent of its role in pro-MMP-2 activation. Dev. Biol. *277*, 255–269.

Page-McCaw, A., Ewald, A.J., and Werb, Z. (2007). Matrix metalloproteinases and the regulation of tissue remodelling. Nat. Rev. Mol. Cell Biol. *8*, 221–233.

Perl, A.K., Wert, S.E., Nagy, A., Lobe, C.G., and Whitsett, J.A. (2002). Early restriction of peripheral and proximal cell lineages during formation of the lung. Proc. Natl. Acad. Sci. USA *99*, 10482–10487.

Petersen, T.H., Calle, E.A., Zhao, L., Lee, E.J., Gui, L., Raredon, M.B., Gavrilov, K., Yi, T., Zhuang, Z.W., Breuer, C., et al. (2010). Tissue-engineered lungs for in vivo implantation. Science *329*, 538–541.

Petrache, I., Natarajan, V., Zhen, L., Medler, T.R., Richter, A.T., Cho, C., Hubbard, W.C., Berdyshev, E.V., and Tuder, R.M. (2005). Ceramide upregulation causes pulmonary cell apoptosis and emphysema-like disease in mice. Nat. Med. *11*, 491–498.

Rawlins, E.L., Okubo, T., Xue, Y., Brass, D.M., Auten, R.L., Hasegawa, H., Wang, F., and Hogan, B.L. (2009). The role of Scgb1a1+ Clara cells in the long-term maintenance and repair of lung airway, but not alveolar, epithelium. Cell Stem Cell *4*, 525–534.

Red-Horse, K., Crawford, Y., Shojaei, F., and Ferrara, N. (2007). Endothelium-microenvironment interactions in the developing embryo and in the adult. Dev. Cell *12*, 181–194.

Rock, J.R., and Hogan, B.L. (2011). Epithelial progenitor cells in lung development, maintenance, repair, and disease. Annu. Rev. Cell Dev. Biol. *27*, 493–512.

Ruoslahti, E., and Rajotte, D. (2000). An address system in the vasculature of normal tissues and tumors. Annu. Rev. Immunol. *18*, 813–827.

Sakaguchi, T.F., Sadler, K.C., Crosnier, C., and Stainier, D.Y. (2008). Endothelial signals modulate hepatocyte apicobasal polazrization in zebrafish. Curr. Biol. *18*, 1565–1571.

Schenk, S., Hintermann, E., Bilban, M., Koshikawa, N., Hojilla, C., Khokha, R., and Quaranta, V. (2003). Binding to EGF receptor of a laminin-5 EGF-like fragment liberated during MMP-dependent mammary gland involution. J. Cell Biol. *161*, 197–209.

Seandel, M., Butler, J.M., Kobayashi, H., Hooper, A.T., White, I.A., Zhang, F., Vertes, E.L., Kobayashi, M., Zhang, Y., Shmelkov, S.V., et al. (2008). Generation of a functional and durable vascular niche by the adenoviral E4ORF1 gene. Proc. Natl. Acad. Sci. USA *105*, 19288–19293.

Shu, W., Jiang, Y.Q., Lu, M.M., and Morrisey, E.E. (2002). Wnt7b regulates mesenchymal proliferation and vascular development in the lung. Development *129*, 4831–4842.

Stratman, A.N., Saunders, W.B., Sacharidou, A., Koh, W., Fisher, K.E., Zawieja, D.C., Davis, M.J., and Davis, G.E. (2009). Endothelial cell lumen and vascular guidance tunnel formation requires MT1-MMP-dependent proteolysis in 3-dimensional collagen matrices. Blood *114*, 237–247.

Stratman, A.N., Schwindt, A.E., Malotte, K.M., and Davis, G.E. (2010). Endothelial-derived PDGF-BB and HB-EGF coordinately regulate pericyte recruitment during vasculogenic tube assembly and stabilization. Blood *116*, 4720–4730.

Stripp, B.R., and Reynolds, S.D. (2008). Maintenance and repair of the bronchiolar epithelium. Proc. Am. Thorac. Soc. *5*, 328–333.

Vaporciyan, A.A., DeLisser, H.M., Yan, H.C., Mendiguren, I.I., Thom, S.R., Jones, M.L., Ward, P.A., and Albelda, S.M. (1993). Involvement of platelet-endothelial cell adhesion molecule-1 in neutrophil recruitment in vivo. Science *262*, 1580–1582.

Voelkel, N.F., Vandivier, R.W., and Tuder, R.M. (2006). Vascular endothelial growth factor in the lung. Am. J. Physiol. Lung Cell. Mol. Physiol. *290*, L209–L221.

Wang, Y., Nakayama, M., Pitulescu, M.E., Schmidt, T.S., Bochenek, M.L., Sakakibara, A., Adams, S., Davy, A., Deutsch, U., Lüthi, U., et al. (2010). Ephrin-B2 controls VEGF-induced angiogenesis and lymphangiogenesis. Nature *465*, 483–486.

Warburton, D., El-Hashash, A., Carraro, G., Tiozzo, C., Sala, F., Rogers, O., De Langhe, S., Kemp, P.J., Riccardi, D., Torday, J., et al. (2010). Lung organogenesis. Curr. Top. Dev. Biol. *90*, 73–158.

White, A.C., Lavine, K.J., and Ornitz, D.M. (2007). FGF9 and SHH regulate mesenchymal Vegfa expression and development of the pulmonary capillary network. Development *134*, 3743–3752.

Whitsett, J.A., Wert, S.E., and Weaver, T.E. (2010). Alveolar surfactant homeostasis and the pathogenesis of pulmonary disease. Annu. Rev. Med. *61*, 105–119.

Yamamoto, H., Yun, E.J., Gerber, H.P., Ferrara, N., Whitsett, J.A., and Vu, T.H. (2007). Epithelial-vascular cross talk mediated by VEGF-A and HGF signaling directs primary septae formation during distal lung morphogenesis. Dev. Biol. *308*, 44–53.

Yana, I., Sagara, H., Takaki, S., Takatsu, K., Nakamura, K., Nakao, K., Katsuki, M., Taniguchi, S., Aoki, T., Sato, H., et al. (2007). Crosstalk between neovessels and mural cells directs the site-specific expression of MT1-MMP to endothelial tip cells. J. Cell Sci. *120*, 1607–1614.

Zhang, Y., Goss, A.M., Cohen, E.D., Kadzik, R., Lepore, J.J., Muthukumaraswamy, K., Yang, J., DeMayo, F.J., Whitsett, J.A., Parmacek, M.S., and Morrisey, E.E. (2008). A Gata6-Wnt pathway required for epithelial stem cell development and airway regeneration. Nat. Genet. *40*, 862–870.